ENVIRONMENTAL RESEARCH
LETTERS

LETTER • OPEN ACCESS

Concurrent increases in winter precipitation and summer wildfire risk in a warming Alaska

To cite this article: Jueun Lee *et al* 2025 *Environ. Res. Lett.* **20** 104059

ENVIRONMENTAL RESEARCH
LETTERS

OPEN ACCESS

RECEIVED
27 June 2025

REVISED
22 August 2025

ACCEPTED FOR PUBLICATION
8 September 2025

PUBLISHED
23 September 2025

LETTER

Concurrent increases in winter precipitation and summer wildfire risk in a warming Alaska

Jueun Lee[1], S-Y Simon Wang[2], Seok-Woo Son[3], Daehyun Kim[3,4], Jee-Hoon Jeong[5], Hyungjun Kim[6] and Jin-Ho Yoon[1,*]

[1] Department of Environment and Energy Engineering, Gwangju Institute of Science and Technology, Gwangju, Republic of Korea
[2] Department of Agronomy, Kasetsart University, Bangkok, Thailand
[3] School of Earth and Environmental Sciences, Seoul National University, Seoul, Republic of Korea
[4] Department of Atmospheric and Climate Science, University of Washington, Seattle, WA, United States of America
[5] Department of Environment and Energy, Sejong University, Seoul, Republic of Korea
[6] Moon Soul Graduate School of Future Strategy, Korea Advanced Institute of Science and Technology, Daejeon, Republic of Korea
[*] Author to whom any correspondence should be addressed.

E-mail: yjinho@gist.ac.kr

Keywords: wildfire, seasonal cascade, compound event, atmospheric circulation

Supplementary material for this article is available online

Abstract

Alaska is experiencing simultaneous trends of increased winter wetness and heightened summer fire risk due to global warming, leading to more frequent wildfires and greater unpredictability in fire behavior in recent decades. Large-ensemble simulations show that warming drives distinct seasonal changes: in winter, an intensified ridge over the western U.S. enhances moisture transport to Alaska, increasing precipitation while promoting vegetation growth near the Alaska Range. In summer, rising temperatures intensify the fire weather index signaling greater wildfire potential and increase lightning activity. Although the links among these complex seasonal changes remain difficult to validate, temporal overlap—enhanced vegetation growth followed by more fire-conducive weather, and associated increase in lightning could collectively heighten wildfire risk. The robustness of our large-ensemble simulations provides compelling evidence for these cascading effects. Extreme lightning-driven events, such as the Swan Lake Fire, represent the emerging pattern in Alaska's evolving fire regime. The concurrent rise in winter wetness and summer fire conditions underscore the urgent need for adaptive fire management strategies that address these interconnected climate drivers.

1. Introduction

Global warming has intensified wildfires in Alaska, escalating their frequency and severity while expanding burned areas and hindering containment efforts (Kasischke *et al* 2010, Kelly *et al* 2013, Young *et al* 2016, Scholten *et al* 2021, Phillips *et al* 2022). Alaska's wildfire activity is closely linked to dry lightning events, which have become a primary ignition source for these destructive fires (Veraverbeke *et al* 2017, Chen *et al* 2021, Janssen *et al* 2023, Perez-Invernon *et al* 2023). Recent incidents, such as the 2019 Swan Lake Fire in the Kenai Peninsula and persistent outbreaks throughout 2024 in Fairbanks, highlight this growing concern. Despite the clear coherence between the warming climate and the increased wildfire crisis, our understanding of the complex interplay between winter rains, lightning events, and large-scale wildfire occurrences in Alaska remains limited, restricting our ability to develop future wildfire management strategies in this rapidly changing climate.

Climate-driven shifts in Alaska's hydrological cycle have significantly changed the region's fire ecology (Walker *et al* 2019), by modifying the interactions with fuel loads and ignition sources. As warming trends lead to increased rainfall and snowmelt (Qin *et al* 2020), subsequent changes in soil moisture regimes are modifying vegetation composition (Wrona *et al* 2016, Bjorkman *et al* 2018, Douglas *et al* 2020) which in turn influence fuel load distributions (Kim *et al* 2024). However, the intricate relationship between shifting vegetation patterns, summer climate, and wildfire risk remains insufficiently understood, adding uncertainty to fire climate projections. While previous studies have identified various factors contributing to Alaska's wildfires, we still lack a cohesive framework that captures the interplay between large-scale circulation and the regional climate evolving fire ecosystem. This critical gap in our understanding hinders the development of adaptive management under global warming, leaving Alaska's ecosystems and communities vulnerable to unprecedented shifts in fire regimes.

In response to these knowledge gaps, this study utilizes multi-ensemble simulations to analyze the temporal cascading effects of seasonally distinct precipitation changes, vegetation growth shifts, extreme lightning probability, and fire-conducive weather conditions in Alaska. We focus particularly on the increasing co-occurrence of winter precipitation and subsequent summer fire risk and explore potential connections among these concurrent phenomena may have. Thus, this study aims to elucidate how the projected warming climate influences these concurrent seasonal changes and to offer an integrative perspective on utilizing these relationships as predictive indicators for Alaskan wildfire risk.

2. Materials and methods

2.1. Observational and Multi-model datasets for water cycle and fire weather index (FWI) metrics

To calculate changes in the climatology around Alaska for the past 80 years (1941–2020), we primarily obtained data from the ECMWF Reanalysis v5 (ERA5) (Hersbach *et al* 2020). For observational changes in the leaf area index (LAI), we employed the global inventory modeling and mapping studies (GIMMS) LAI4g dataset (Cao *et al* 2023).

For future scenarios of each variable, we used the 50 smoothed biomass-burning members from the Community Earth System Model 2 Large Ensemble (CESM2 LENS) datasets (Rodgers *et al* 2021). The CESM2 LENS is a fully coupled configuration spanning 1850–2100. Each ensemble member is initialized using CMIP6 historical climate forcings until 2014, after which projections are based on the SSP370 future radiative forcing scenario. We focused particularly on the 50 members with smoothed biomass burning to mitigate the high sensitivity of biomass burning to air temperature and sea ice changes, which could affect FWI calculations (DeRepentigny *et al* 2022). To further explore the role of anthropogenic greenhouse gas (GHG) forcing, we utilized 15 members of CESM2 GHG single forcing simulations (Simpson *et al* 2023). In these simulations, all forcings except GHG are fixed at their 1850s values, allowing only the GHG forcing to evolve up to 2050. This approach enables us to isolate and examine the specific response to GHG forcing. Overall, we aligned the future period (TF) up to 2050 in both CESM2 LENS and GHG single forcing simulation.

Based on the CESM2 simulations dataset, total precipitation (PRECT) and latent heat flux (LHFLX) were used to represent the surface net water flux equivalent, and convective available potential energy (CAPE) was used for inferring lightning probability (Peterson *et al* 2010, Romps *et al* 2014, 2018). However, the LAI value was treated differently from other atmospheric model-based output variables. The monthly total projected LAI was taken from the community land model (CLM) output, derived from 30 smoothed biomass-burning members of the CESM2 LENS. To calculate the daily FWI which represent the burned area and fire occurrence frequency (Bedia *et al* 2015, Abatzoglou *et al* 2018, Fox *et al* 2018, Touma *et al* 2021) from CESM2, we used daily maximum temperature (TREFHTMX), PRECT, reference height relative humidity (RHREFHT), and surface wind speed (WSPDSRFAV). Using the average relative humidity instead of the daily minimum relative humidity does not significantly affect the calculated FWI value over Alaska (Quilcaille *et al* 2023). Therefore, it is acceptable to use the RHREFHT in this study. The FWI was initiated in 1935 with a 5 year spin-up period, and data from 1940 onward were used for this study. The 15 GHG single forcing run members were consistently used across all variables.

To validate CESM2 FWI changes, we employed a multi-model approach using five CMIP6 Earth system models (ESMs) datasets from ACCESS-ESM1-5 (Ziehn *et al* 2020), CanESM5 (Swart *et al* 2019), EC-Earth3 (Döscher *et al* 2022), MIROC6 (Tatebe *et al* 2019), and MPI-ESM1-2-LR (Mauritsen *et al* 2019)—with an FWI-based annual fire risk indicator specifically FWI_{95}, which represents the annual number of days exceeding the 95th percentile threshold established from the historical period and reflects the probability of large-scale fire occurrence (Quilcaille *et al* 2023). We specifically selected large-ensemble ESMs to ensure a fair comparison with CESM2, utilizing 20 members each from individual models with historical and SSP245 scenarios that are available from www.research-collection.ethz.ch/handle/20.500.11850/583391. For FWI_{95} days in figure 1, the reference period was set to 1850–1900, which differs from the reference period in ERA5 and CESM2 simulations (T1, 1941–1970). Therefore, since the FWI baseline is further in the past, the FWI_{95} days in CMIP6 ESMs may be overestimated compared to ERA5 and CESM2 simulations. Precipitation flux changes were calculated similarly.

2.2. Threshold of individual extreme events and concept of compound events

This study applied different thresholds for calculating compound events involving FWI and CAPE versus those involving surface net water flux (P–E)

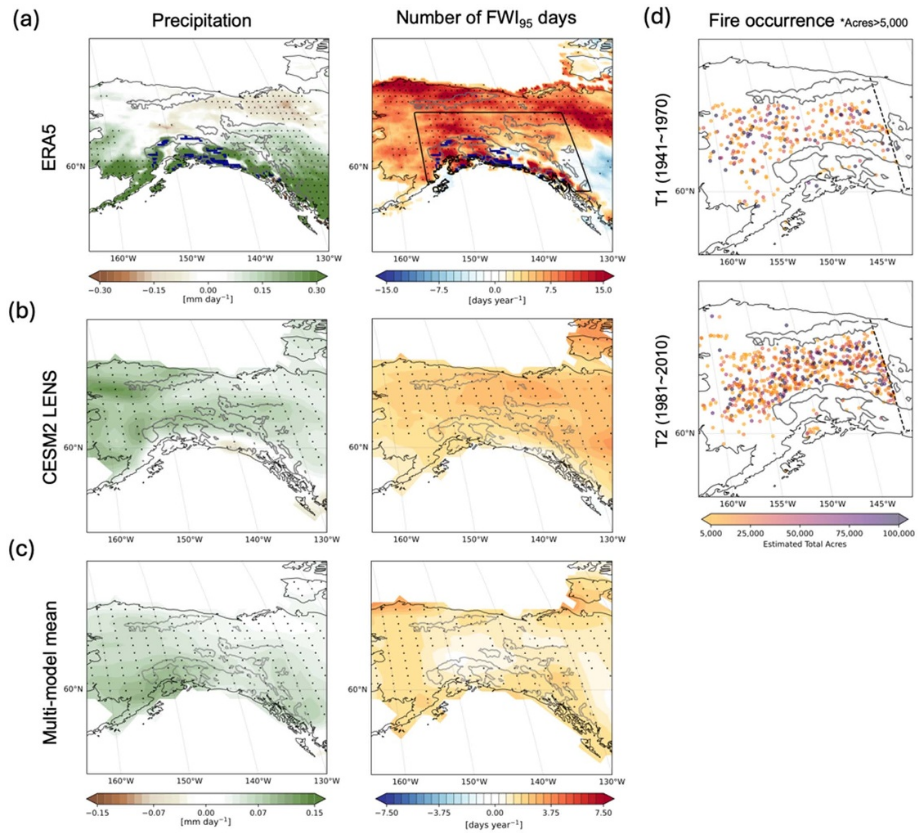

Figure 1. Enhanced precipitation and intensified fire risk potential in Alaska during the past decades. Annual mean differences in precipitation flux and fire risk potential indicator between the earlier 30 years (T1, 1941–1970) and the recent 30 years (T2, 1981–2010) from (a) ERA5 dataset, (b) CESM2 LENS, and (c) CMIP6 large-ensemble Earth System Model's mean (ACCESS-ESM1-5, CanESM5, EC-Earth3, MIROC6, and MPI-ESM1-2-LR). The number of FWI95 days is calculated by establishing the 95th percentile threshold for each ensemble during the reference period, then counting the number of days exceeding this threshold. (d) Actual wildfire occurrence exceeding 5000 estimated total acres from T1 to T2 periods. Significant differences are dotted in all figures ($p < 0.05$), and gray lines represent topography above 1000 m representing the major mountain ranges around Alaska. The blue areas in figure 1(a) represent the glacier areas in Alaska.

and LAI. For both CESM2 LENS and GHG single forcing runs, thresholds were determined by considering all ensemble members collectively for each individual experiment, thereby reducing ensemble dependency and enabling more consistent comparisons. FWI and CAPE extreme cases were defined as values exceeding the 99th percentile, focusing on extreme events. This threshold is stricter than the FWI_{95} definition used in figure 1, allowing us to exclusively examine conditions with a very high probability of actual fire occurrence in model projection. In contrast, for P–E and LAI, we considered values exceeding 1 standard deviation above the mean, representing consistently high values rather than extreme cases. To account for temporal relationships, we counted occurrences of extreme CAPE ($CAPE_{99}$) within 7, 14, and 30 d following extreme FWI (FWI_{99}) events for short-term compound events. For long-term compound events, we counted occurrences of high greenness (LAI_{1std}) events within 6, 9, and 11 months following high wetness events ($P–E_{1std}$). This approach allows us to capture both short-term extreme event relationships and longer-term ecosystem responses to changes in the water cycle.

2.3. Wet and dry seasons in Alaska

Alaska's climate is characterized by distinct seasonal variability, with wet winters and subsequent dry seasons from late spring to summer. Most precipitation in Alaska, particularly in southern regions, is concentrated during the winter months. In contrast, summer months are becoming progressively drier with a corresponding increase in wildfire occurrence. Previous studies have typically defined December to February as winter and June to August as summer (Cahoon *et al* 2022, Masrur *et al* 2022). However, some studies suggest that fire activity and related climatic conditions span broader temporal windows (Jolly *et al* 2015, Senande-Rivera *et al* 2022), indicating that seasonal patterns may be evolving under climate change. In this study, rather than limiting wet and dry seasons to conventional winter and summer periods, we define seasonal boundaries based on the observed seasonality during the historical period (T1, 1941–1970) and examine how these patterns change in the present (T2, 1981–2010) and future (T3, 2021–2050) periods. Accordingly, we define the wet season as October to February and the dry season as May to September, reflecting Alaska's distinct seasonal precipitation and fire activity patterns.

3. Results

3.1. Intensifying winter wetness and summer fire-conducive weather conditions in Alaska

To diagnose the historical annual fire risk potential, we employed an established indicator based on FWI_{95} and defined climatological periods with three 30 year time intervals: T1 (1941–1970) representing the historical baseline, T2 (1981–2010) capturing recent changes, and TF (2021–2050) projecting future conditions. Our analysis reveals that Alaska's annual mean precipitation flux and fire weather conditions have significantly changed over the past decades, becoming more severe (figure 1(a)). These regional variations are evident across Alaska. Specifically, southern Alaska and mountain ranges exhibit more precipitation, suggesting a clear tendency toward wetter conditions, while interior regions of Alaska have shown muted changes in precipitation patterns. Meanwhile, the number of days exceeding FWI_{95} shows increasing tendencies across the southern and near Alaska mountain ranges as a river basin area. Additionally, calculating changes in large-scale actual fire counts and estimated total burned areas exceeding 5000 acres during the historical period reveals increasing patterns across Alaska's interior and southern regions (figure 1(d)). Comparing T1 to T2 periods shows more than 10 million additional acres burned and approximately 350 more fire occurrences, confirming the increasingly severe conditions facing the region (figure S1).

These historical trends are partially captured in southern Alaska by simulations of historical changes (T2 minus T1) from CMIP6 large-ensemble ESMs, but biases exist in simulating conditions for higher-latitude regions of Alaska (figure 1(c)). In figure S2, the individual five CMIP6 large-ensemble ESMs (ACCESS-ESM1-5, CanESM5, EC-Earth3, MIROC6, and MPI-ESM1-2-LR) also partially capture the observational results. These models show relatively similar patterns to ERA5 but exhibit considerable biases in interior regions within Alaska. In contrast, the spatial features of CESM2 LENS in reproducing observed historical patterns demonstrate its capability to simulate the characteristics of fire-prone environments around the Alaska mountain range and interior of Alaska, showing good agreement with ERA5 results (figure 1(b)).

We extend our analysis based on these historical patterns to examine future changes (TF minus T1). The increasing tendency in both the annual mean of precipitation flux and fire weather indicator continues and intensifies in future projections from both CMIP6 ESMs and CESM2 LENS (figures 2(a), (c) and S3). In particular, the ensemble means of CESM2 GHG single forcing runs demonstrate a clear intensification trend that becomes more pronounced in the future (figure 2(b)). Under the GHG forcing, we find a more distinct wetness and fire weather trend in Alaska, consistent with and reinforcing the observed historical patterns. This suggests a striking paradox in Alaska's climate projection. While southern regions may experience increased annual moisture conditions, the overall fire risk is escalating throughout Alaska. These concurrent trends are predominantly accelerated by anthropogenic GHG forcing, likely involving factors such as surface temperature increases and enhanced vegetation growth. Given CESM2 LENS's demonstrated skill in capturing historical spatial patterns, these large-ensemble simulations provide a comprehensive view of Alaska's evolving fire weather vulnerability. While individual CMIP6 ESMs show inconsistent projections, this variability suggests that GHG forcing potentially reinforces the role of anthropogenic warming as the primary driver.

Since actual wildfire occurrence requires both elevated FWI and accompanying vegetation and ignition sources, this study focuses on seasonal variations of key variables: P–E (surface water flux), LAI (vegetation proxy), FWI, and CAPE (lightning probability indicator), which are primary fire components in Alaska. To quantify historical seasonality changes, P-E and FWI were calculated using weighted area averages for inland regions (57°–67° N, 155°–130° W, box plot in figure 1(a)), excluding glacier areas (figure 1(a), masked in blue). CESM2 LENS closely reproduces the seasonality in ERA5 and its amplification (figure S4), as a key criterion for our expected model skill. Therefore, in this study, we define the wet season as October to February and the dry season as May–September.

Southern Alaska and mountain ranges have become increasingly wet (figure 1(a), precipitation) while FWI has intensified over Alaska (figure S5, FWI). These changes are accompanied by warmer near-surface temperatures and increased snow melting in these regions (figure S5, T2m, Snow melt). Additionally, the lightning probability, as represented by CAPE has increased in Alaska (figure S5). The concurrent, increased LAI confirms enhanced vegetation growth (figure S6). These increased precipitation and snow melting near the Alaska mountain ranges may contribute to enhanced water availability in surrounding areas through mountain river basins, potentially supporting vegetation growth in the following months. These watershed regions also experience increasing fire weather conditions, demonstrating that mountain precipitation and fire-prone

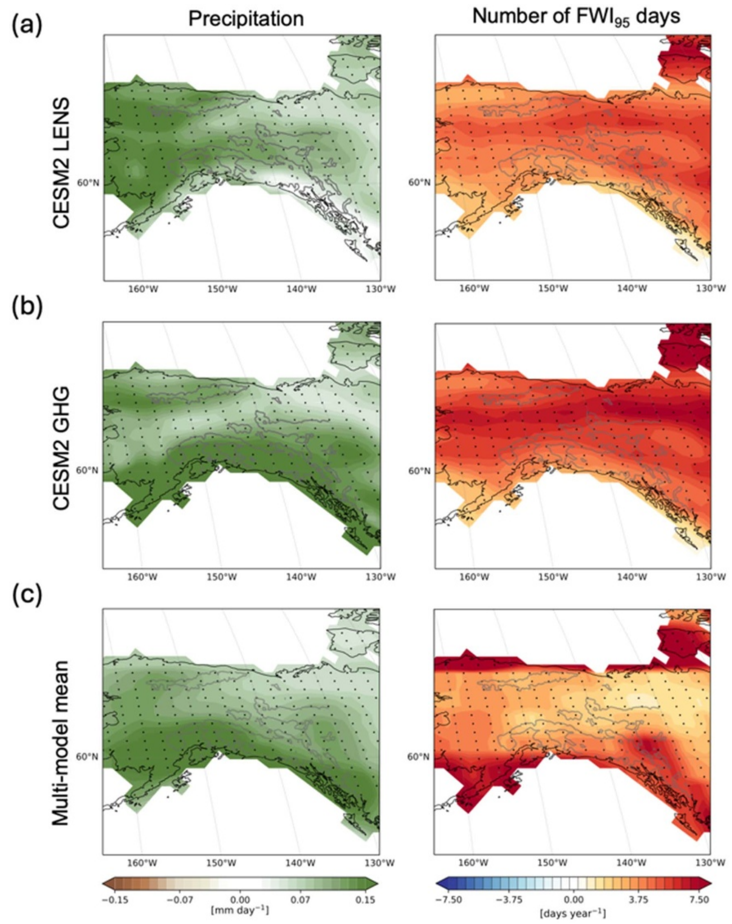

Figure 2. Projected future increasing wetness and worsening fire weather conditions in Alaska driven by anthropogenic GHG forcing. Similar plot to figure 1 but for the difference between the historical (T1) and future period (TF, 2021–2050) from (a) CESM2 LENS, (b) CESM2 greenhouse gas (GHG) single forcing experiments, and (c) CMIP6 large-ensemble Earth system model's mean for SSP245 scenario. Significant differences are dotted in all figures ($p < 0.05$), and gray lines represent topography above 1000 m representing the major mountain ranges around Alaska.

areas could share geographic relationships through common river basin systems (Bennett *et al* 2015). We also examined the changes in seasonality of root zone or equivalent (0–100 cm) soil water content from ERA5 and global land data assimilation system (GLDAS) models (Noah LSM, CLM, and VIC) over the historical period confirms a modest increase from CLM and ERA5 in soil moisture during spring and early summer but other models show muted response (figure S7).

Based on CESM2 LENS, the future projections reveal an amplification of the seasonality of each variable. As winter P–E increases, the following dry season's LAI increases simultaneously. Similarly, the FWI in the dry season (May to September) increases along with CAPE (figure 3, CESM2 LENS). Notably, the intensification of dry season FWI and CAPE begins as early as May, peaking in June—significantly earlier than the typical summer season onset (June). Rising temperatures and fire weather conditions foster an environment conducive to dry thunderstorms, which generate dry lightning with minimal ground-reaching rainfall due to increased surface evaporation (Price 2009, Kalashnikov *et al* 2022). These temporal shifts create critical overlaps between enhanced vegetation, advanced fire seasons, and increased lightning activity, particularly elevating fire risks in areas with dense summer vegetation. Anthropogenic GHG forcing further amplifies these seasonal changes, with even weak late-season CAPE decreases in CESM2 LENS showing notable increases under GHG forcing (figure 3, CESM2 GHG). This concurrent intensification and altered seasonal sequencing of climate variables point to a cascading process that escalates Alaska's vulnerability to fire-conducive weather.

3.2. Sequential compound climate events heighten Alaska's fire risk

As global warming intensifies, Alaska's seasonal patterns are undergoing noticeable transformations. Winters are becoming increasingly wet (October–February), while subsequent summers face escalating fire risks (May–September) (figure 3). Our study hypothesizes that temporal co-occurrence among

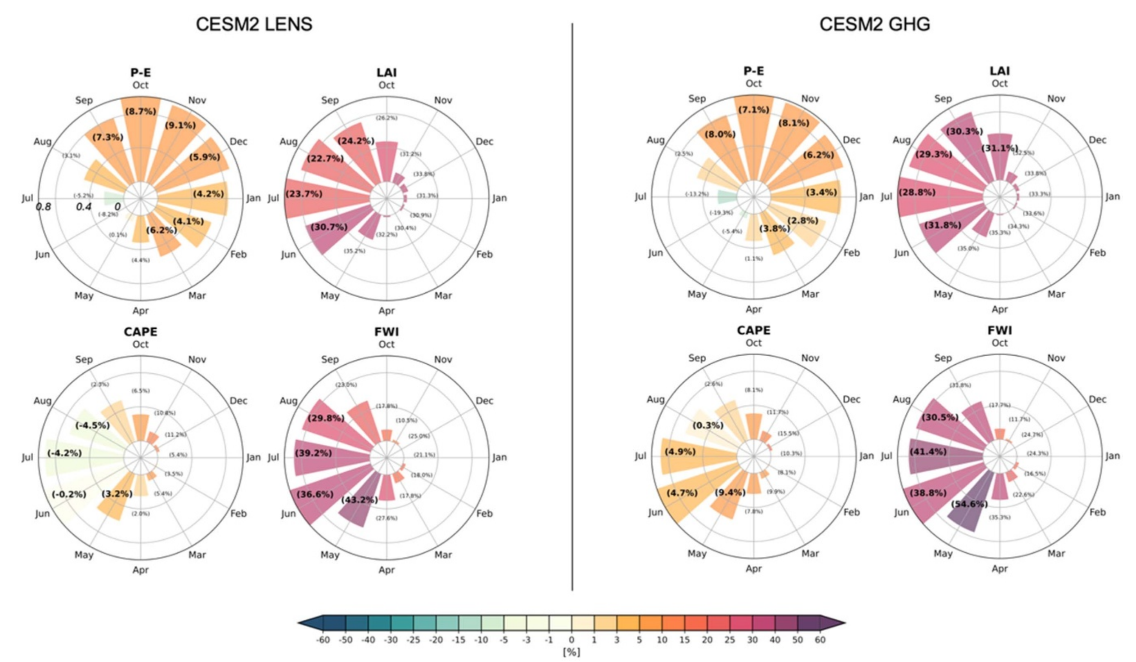

Figure 3. GHG forcing amplifies the seasonality of fire occurrence variables. The normalized mean of P–E (total precipitation minus surface latent heat flux), LAI, CAPE, and FWI for the T1 (in a magnitude of the bar), and their respective change in the TF (shading) from CESM2 LENS and GHG single forcing datasets. Seasonality is calculated using a weighted area average over the inland regions near Alaska (57°–67° N, 155°–130° W), considering only land grid points and excluding glacier areas as shown in figure 1(a). Bold values indicate the relative percent change for each variable in its representative season.

seasonal climate variables is rising, thereby elevating the probability of concurrent high-risk fire conditions in Alaska.

We first examine sequential (or time-lagged) compound events among seasonally distinct variables to reveal patterns in the projected fire-prone condition across Alaska. Utilizing CESM2 LENS and GHG single forcing runs, we analyze changes across interior Alaska in two types of compound events: extreme fire weather conditions paired with extreme lightning probability, and wetness coupled with vegetation growth (figure 4). Each compound event reveals distinctive climate-related vulnerabilities. Figure 4(a) represents the dry season (May–September) and demonstrates changes in the frequency of compound events linking extreme FWI with subsequent extreme CAPE days. These events are analyzed within 7, 14, and 30 d, capturing short- to medium-term fire risk escalation. If extreme lightning occurs shortly after the formation of extreme fire-conducive weather conditions, highly favorable conditions for wildfire ignition can develop. Indeed, figure 4(b) addresses the relationship between wet season (October–February) P–E and subsequent dry season LAI, examining compound events over longer periods of 6, 9, and 11 months. This illustrates us to assess how increased surface moisture availability might influence vegetation growth and consequent fire fuel accumulation in a subsequent dry season.

Each compound event employs different thresholds to capture specific aspects of fire risk. FWI and CAPE focus on extreme cases, considering only values above the 99th percentile (FWI_{99} and $CAPE_{99}$). Unlike the previous analysis using individual ensemble 95th percentiles (figures 1 and 2, FWI_{95}), we applied a uniform 99th percentile threshold across all ensembles for FWI and CAPE to focus on truly extreme events with very high fire occurrence probability. P–E and LAI thresholds were set at one standard deviation above the mean to capture overall increases in wetness and vegetation growth (see methods). These settings allow examination of how long-term vegetation changes and short-term extreme fire weather can create hazardous wildfire conditions in Alaska.

Across Alaska, the future projections from the CESM2 LENS simulations indicate an increasing frequency of compound events involving extreme FWI and extreme CAPE. Concurrently, compound events characterized by large P–E and LAI show an increasing tendency (figure 4, CESM2 LENS). Furthermore, the frequency of compound events increases as the lag time extends, indicating that each compound event persistently operates under extended time intervals. Specifically, after Alaska's winters become wetter, this might trigger rapid vegetation growth from 6 to 9 months following this wet period, with the frequency of these compound events steadily increasing up to 11 months. The period of increased LAI overlaps with the dry season when FWI and CAPE activity are high. During this season, extreme fire weather conditions form, and there is a high probability of extreme lightning occurrence within a month. This suggests the potential implementation of a 'High Fire

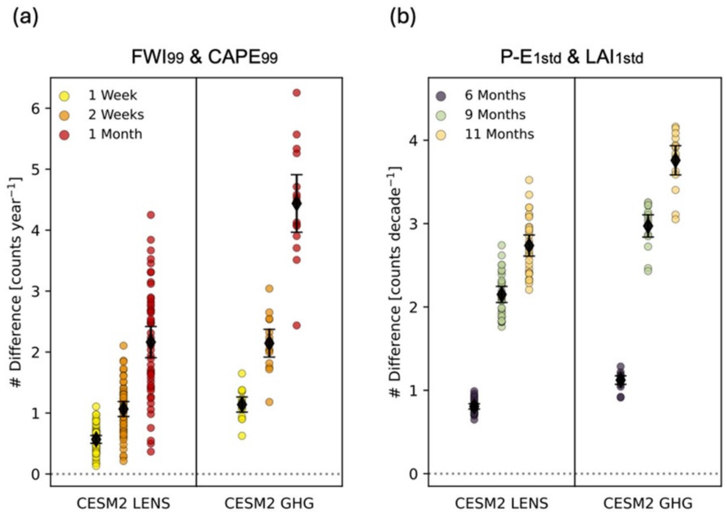

Figure 4. Heightened fire-prone compound event frequency in Alaska. (a) Changes in compound event frequency from T1 to TF: extreme fire weather during the dry season (May–September) followed by extreme CAPE days (within 7, 14 d, and one month). (b) Changes in compound event frequency from T1 to TF: wet season (October–February) wetness followed by dry season vegetation growth (within 6, 9, and 11 months). In both panels, black marks represent ensemble means, with error bars indicating the 1 standard deviation range. Both analyses use CESM2 LENS and GHG single forcing datasets, with the left panel based on daily data and the right panel on monthly data. Thresholds are determined by considering historical periods (T1) for all ensemble members together and then applied to each ensemble individually. The 99th percentile is used for fire weather/CAPE events and 1 standard deviation for P-E/LAI events. Calculations are based on 50 LENS members for FWI and CAPE, while for P-E and LAI, 30 LENS members were used, selecting P-E data matching the ensemble numbers of the available monthly LAI data. The frequency of compound events is the weighted-area average from the domain defined in figure 3.

Alert Period' lasting for up to one month following extreme FWI days, calling for heightened vigilance and preemptive fire management strategies. This synchronicity between compound events is further amplified by anthropogenic GHG forcing (figure 4, CESM2 GHG), suggesting that human activities are likely to cause more frequent occurrences of these fire-prone conditions in the future.

Notably, Alaska's population is concentrated in southern regions and river basins near the Alaska ranges (Anchorage, Kenai Peninsula, Fairbanks). Spatial analysis reveals pronounced intensification of both compound event types in these southern mountain areas (figures S8 and S9), suggesting that fire-prone conditions are projected to occur more frequently in populated regions, potentially posing greater risks to Alaskan residents and necessitating preventive action.

3.3. Increasing co-variability of fire risk factors

The increasing frequency of fire risk compound events in Alaska is notable. However, an understanding of the evolving co-variability between climate variables can serve as evidence for projecting future fire hazards. Thus, this study further aims to examine these covariances between climate variables to enhance the predictability of fire risks. We focus on temporal co-occurrence patterns rather than establishing causal mechanisms between seasonal processes, which will require further investigation to fully understand the underlying connections.

We utilized a 30 year sliding window to capture multi-decadal climate variability. The 30 year sliding covariance between FWI and CAPE (figure 5(a)) and between P–E and LAI (figure 5(b)) shows a marked increase over time. Specifically, the covariance between FWI and CAPE occurring 3 d after the FWI event begins to show a significant increase in future projections. This enhanced covariance persists up to 21 d post-FWI, before showing a declining trend beyond one month. Similarly, for the P-E and LAI relationship, a strong co-variability emerges 7 months after the P–E event, persisting for up to 10 months, and then weakening after 11 months (figure 5, CESM2 LENS).

The findings indicate a progressive intensification of the covariance between the elements of these compound events as future scenarios unfold. Strikingly, an increasing covariance pattern is observed not only within each compound event but also between FWI and LAI (figure S10). While the co-variability strengthens in future projections even at concurrent time points, it becomes particularly pronounced for LAI one month after FWI formation. This 'one-month' temporal interval holds significant importance in the fire-prone environment system. The extreme CAPE tends to form within one month of extreme FWI occurrence (figure 4(a)), and the covariance between FWI and CAPE within this one month also intensifies markedly in future projections (figure 5(a)). The 30 year covariance of FWI and LAI reveals their climatological relationships, indicating that an increase in FWI does not necessarily lead to

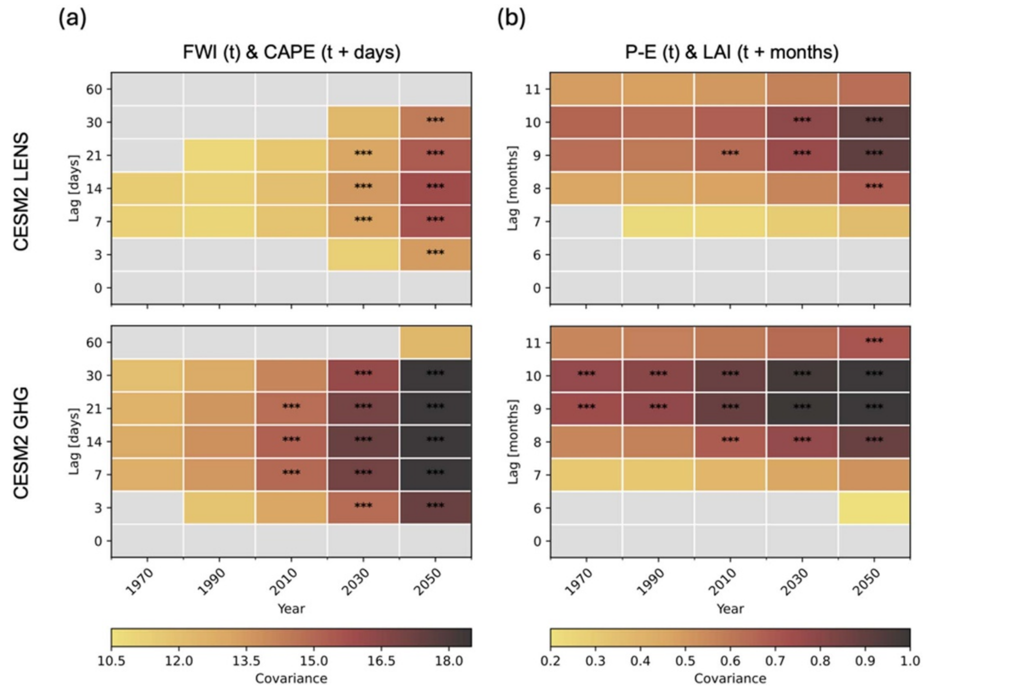

Figure 5. Increasing co-variability through temporal cascading in fire-prone compound events. The 30 year temporal lag covariance between two climate variables characterizes each compound event. (a) Covariance between daily FWI and CAPE after representative days. (b) Covariance between monthly P–E and LAI after representative months. For both figures, the covariance is calculated over 30 years, starting from 30 years before the specified year on the *x*-axis. The mark (***) indicates covariances where more than two-thirds of the ensemble members show statistically significant values at the $p < 0.001$ level. Grey areas represent covariances that are not statistically significant ($p \geqslant 0.05$). Statistical significance was determined using a permutation test, which directly tests the null hypothesis that there is no temporal relationship between the two variables. This was done by randomly shuffling the following variables (CAPE and LAI) 5000 times, disrupting only the temporal relationship while maintaining other statistical characteristics of the raw data.

actual fire occurrence and subsequent LAI decrease. Rather, the positive relationships with LAI increasing one month after FWI occurrence are interlinked with the relationship with CAPE, which surges between two weeks to one month after the cause while summer LAI being the FWI increases. Consequently, this implies that extreme CAPE-induced lightning potential during this critical period effectively becomes a source for conflagrations.

The intensified co-variability under the influence of GHG forcing (figure 5, CESM2 GHG and figure S10, CESM2 GHG), in which more areas meet robust significance levels, shows that increased compound event frequency is coupled with the substantial role of anthropogenic climate change in this process underscores how human activities are accelerating the formation of a more extreme fire regime in Alaska. This new regime is unfolding as global warming amplifies the seasonality of each variable and tightens their temporal sequencing. Long-term wildfire management strategies in the region. By leveraging these findings, we could implement proactive prevention measures, potentially mitigating the exacerbation of fire hazards in the coming decades.

3.4. The role of large-scale climate dynamics

The observed shift towards wetter Alaska winters is particularly influenced by amplification of the upper troposphere ridge over western North America (Lee *et al* 2024, 2025). As global temperatures rise, the upper tropospheric stream function intensifies, exhibiting North American Winter Dipole (NAWD) characteristics with significant implications for regional weather extremes (Screen and Simmonds 2014, Wang *et al* 2014, 2015, 2017, Simpson *et al* 2015, Chien *et al* 2019, Voelker *et al* 2019). During exceptionally wet Alaskan winters, a slightly eastward-shifted ridge acts as a gateway for Pacific moisture influx into southern Alaska (figure S11). In summer, the increasingly severe fire weather conditions and warmer near-surface temperatures coincide with moisture-laden low-level troposphere southerly winds from the Pacific (figure S12). These winds, upon encountering the Alaska Range, potentially enhance uplift and form cumulonimbus clouds, destabilizing upper tropospheric air parcels and creating favorable conditions for dry lightning (Trapp *et al* 2007, Farukh and Hayasaka 2012, Abatzoglou and Williams 2016). While rain accompanies this lightning, warmer surface conditions and evaporation result in lightning primarily reaching the ground, potentially igniting large-scale wildfires in expanded summer vegetation.

4. Summary and discussion

This study reveals a climate-driven cascade wherein global warming intensifies Alaska's winter precipitation alongside heightened lightning-caused wildfire risk during subsequent dry seasons. Central to these observations is the enhanced vegetation growth, or 'greening', which provides more fuel for wildfires. Under global warming, rising temperatures accelerate the accumulation of snowmelt in surrounding mountain ranges, with the resulting water flowing through river basins during subsequent spring and late summer (Park *et al* 2024), contributing to vegetation growth (Musselman *et al* 2021, Koch *et al* 2022, Blaskey *et al* 2023, 2025). Concurrently, summer warming intensifies fire-conducive weather and enhances lightning probability while advancing the onset of fire seasons. The temporal overlap of enhanced vegetation growth, extended fire-prone weather, and increased lightning activity later in summer collectively amplifies wildfire risks. GHG-induced future warming amplifies this co-variability.

Our study projects an intensification of fire-conducive events in Alaska, with increasing frequency of compound events where multiple climate factors converge, creating high-risk fire conditions. Notably, the co-variability among key variables such as winter precipitation, subsequent summer vegetation growth, fire weather conditions, and lightning probability is strengthening under anthropogenic GHG forcing. While specific mechanistic linkages require further investigation, the implicated physical connection between increased winter precipitation and elevated summer wildfire risk demands more comprehensive examination. Instead, these phenomena appear to emerge as parallel responses to the common external forcing of anthropogenic warming. Even so, their temporal coincidence creates a potentially more hazardous fire environment. Whether causally connected or independently responding to climate change, this synchronous occurrence may substantially elevate Alaska's wildfire risk. These concurrent trends underscore the need for adaptive fire management strategies as human-driven global warming escalates.

Data availability statement

All meteorological data utilized in this study are publicly available. The ERA5 datasets can be accessed at www.ecmwf.int/en/forecasts/dataset/ecmwf-reanalysis-v5. The Community Earth System Model 1 Large Ensemble Community Project (CESM1 LENS) datasets are available at www.cesm.ucar.edu/community-projects/lens/data-sets, and the CESM1 Single Forcing Large Ensemble Project data can be found at www.cesm.ucar.edu/working-groups/climate/simulations/cesm1-single-forcing-le. CMIP6 ESMs, including historical and ssp245 scenarios simulations, can be obtained from www.research-collection.ethz.ch/handle/20.500.11850/583391. This study employed Python, NCAR Command Language (NCL), Climate Data Operators (CDO), and Fortran for data processing and statistical analyses.

All data that support the findings of this study are included within the article (and any supplementary files).

Acknowledgment

This work was supported by the National Research Foundation of Korea (2021R1A2C1011827), by the Korea Environment Industry & Technology Institute (KEITI) through "Climate Change R&D Project for New Climate Regime", funded by Korea Ministry of Environment (MOE) (RS-2022-KE002160), and by the Korean Meteorological Agency under the grant KMI2018-07010. HK was supported by the National Research Foundation of Korea(NRF) grant funded by the Korea Government(MSIT)(RS-2021-NR055516).

Author contributions

Jueun Lee 0009-0007-4061-0347
Conceptualization (equal), Formal analysis (equal), Investigation (equal), Methodology (equal), Software (equal), Visualization (equal), Writing – original draft (equal)

S-Y Simon Wang
Conceptualization (equal), Supervision (equal), Writing – review & editing (equal)

Daehyun Kim 0000-0001-9233-2747
Writing – review & editing (equal)

Jee-Hoon Jeong
Writing – review & editing (equal)

Hyungjun Kim 0000-0003-1083-8416
Writing – review & editing (equal)

Jin-Ho Yoon 0000-0002-4939-8078
Conceptualization (equal), Funding acquisition (equal), Investigation (equal), Resources (equal), Supervision (equal), Writing – original draft (equal), Writing – review & editing (equal)

References

Abatzoglou J T and Williams A P 2016 Impact of anthropogenic climate change on wildfire across western US forests *Proc. Natl Acad. Sci. USA* **113** 11770–5

Abatzoglou J T, Williams A P, Boschetti L, Zubkova M and Kolden C A 2018 Global patterns of interannual climate-fire relationships *Glob. Change Biol.* **24** 5164–75

Bedia J, Herrera S, Gutiérrez J M, Benali A, Brands S, Mota B and Moreno J M 2015 Global patterns in the sensitivity of

burned area to fire-weather: implications for climate change *Agric. For. Meteorol.* **214–215** 369–79
Bennett K E, Cannon A J and Hinzman L 2015 Historical trends and extremes in boreal Alaska river basins *J. Hydrol.* **527** 590–607
Bjorkman A D *et al* 2018 Plant functional trait change across a warming tundra biome *Nature* **562** 57–62
Blaskey D, Cheng Y, Newman A J, Koch J C, Gooseff M N and Musselman K N 2025 Alaskan hydrology in transition: changing precipitation and evapotranspiration patterns are projected to reshape seasonal streamflow and water temperature by midcentury (2035–64) *J. Hydrometeorol.* **26** 613–26
Blaskey D, Koch J C, Gooseff M N, Newman A J, Cheng Y, O'Donnell J A and Musselman K N 2023 Increasing Alaskan river discharge during the cold season is driven by recent warming *Environ. Res. Lett.* **18** 024042
Cahoon S M P, Sullivan P F and Gray A N 2022 Interactions among wildfire, forest type and landscape position are key determinants of boreal forest carbon stocks *J. Ecol.* **110** 2475–92
Cao S *et al* 2023 Spatiotemporally consistent global dataset of the GIMMS leaf area index (GIMMS LAI4g) from 1982 to 2020 *Earth Syst. Sci. Data* **15** 4877–99
Chen Y, Romps D M, Seeley J T, Veraverbeke S, Riley W J, Mekonnen Z A and Randerson J T 2021 Future increases in Arctic lightning and fire risk for permafrost carbon *Nat. Clim. Change* **11** 404–10
Chien Y-T, Wang S-Y S, Chikamoto Y, Voelker S L, Meyer J D D and Yoon J-H 2019 North American Winter dipole: observed and simulated changes in circulations *Atmosphere* **10** 793
DeRepentigny P *et al* 2022 Enhanced simulated early 21st century Arctic sea ice loss due to CMIP6 biomass burning emissions *Sci. Adv.* **8** 1–12
Döscher R *et al* 2022 The EC-Earth3 earth system model for the coupled model intercomparison project 6 *Geosci. Model Dev.* **15** 2973–3020
Douglas T A, Turetsky M R and Koven C D 2020 Increased rainfall stimulates permafrost thaw across a variety of Interior Alaskan boreal ecosystems *npj Clim. Atmos. Sci.* **3** 28
Farukh M A and Hayasaka H 2012 Active forest fire occurrences in severe lightning years in Alaska *J. Nat. Disaster Sci.* **33** 71–84
Fox D M, Carrega P, Ren Y, Caillouet P, Bouillon C and Robert S 2018 How wildfire risk is related to urban planning and fire weather index in SE France (1990–2013) *Sci. Total Environ.* **621** 120–9
Hersbach H *et al* 2020 The ERA5 global reanalysis *Q. J. R. Meteorol. Soc.* **146** 1999–2049
Janssen T A J, Jones M W, Finney D, van der Werf G R, van Wees D, Xu W and Veraverbeke S 2023 Extratropical forests increasingly at risk due to lightning fires *Nat. Geosci.* **16** 1136–44
Jolly W M, Cochrane M A, Freeborn P H, Holden Z A, Brown T J, Williamson G J and Bowman D M 2015 Climate-induced variations in global wildfire danger from 1979 to 2013 *Nat. Commun.* **6** 7537
Kalashnikov D A, Abatzoglou J T, Nauslar N J, Swain D L, Touma D and Singh D 2022 Meteorological and geographical factors associated with dry lightning in central and northern California *Environ. Res. Clim.* **1** 025001
Kasischke E S *et al* 2010 Alaska's changing fire regime—implications for the vulnerability of its boreal forests this article is one of a selection of papers from the dynamics of change in Alaska's boreal forests: resilience and vulnerability in response to climate warming *Can. J. For. Res.* **40** 1313–24
Kelly R, Chipman M L, Higuera P E, Stefanova I, Brubaker L B and Hu F S 2013 Recent burning of boreal forests exceeds fire regime limits of the past 10,000 years *Proc. Natl Acad. Sci. USA* **110** 13055–60
Kim I-W, Timmermann A, Kim J-E, Rodgers K B, Lee S-S, Lee H and Wieder W R 2024 Abrupt increase in Arctic-Subarctic wildfires caused by future permafrost thaw *Nat. Commun.* **15** 7868
Koch J C, Sjöberg Y, O'Donnell J A, Carey M P, Sullivan P F and Terskaia A 2022 Sensitivity of headwater streamflow to thawing permafrost and vegetation change in a warming Arctic *Environ. Res. Lett.* **17** 044074
Lee J, Wang S-Y S, Son S-W, Kim D, Jeong J-H, Kim H and Yoon J-H 2024 Evolving winter atmospheric teleconnection patterns and their potential triggers across western North America *npj Clim. Atmos. Sci.* **7** 63
Lee J, Wang S-Y S, Son S-W, Kim D, Jeong J-H, Kim H and Yoon J-H 2025 Amplification of Northern Hemisphere winter stationary waves in a warming world *npj Clim. Atmos. Sci.* **8** 20
Masrur A, Taylor A, Harris L, Barnes J and Petrov A 2022 Topography, climate and fire history regulate wildfire activity in the Alaskan Tundra *J. Geophys. Res.: Biogeosci.* **127** e2021JG006608
Mauritsen T *et al* 2019 Developments in the MPI-M earth system model version 1.2 (MPI-ESM1.2) and its response to increasing CO(2) *J. Adv. Model. Earth Syst.* **11** 998–1038
Musselman K N, Addor N, Vano J A and Molotch N P 2021 Winter melt trends portend widespread declines in snow water resources *Nat. Clim. Change* **11** 418–24
Park H, Kim Y, Suzuki K and Hiyama T 2024 Influence of snowmelt on increasing Arctic river discharge: numerical evaluation *Prog. Earth Planet. Sci.* **11** 13
Perez-Invernon F J, Gordillo-Vazquez F J, Huntrieser H and Jockel P 2023 Variation of lightning-ignited wildfire patterns under climate change *Nat. Commun.* **14** 739
Peterson D, Wang J, Ichoku C and Remer L A 2010 Effects of lightning and other meteorological factors on fire activity in the North American boreal forest: implications for fire weather forecasting *Atmos. Chem. Phys.* **10** 6873–88
Phillips C A, Rogers B M, Elder M, Cooperdock S, Moubarak M, Randerson J T and Frumhoff P C 2022 Escalating carbon emissions from North American boreal forest wildfires and the climate mitigation potential of fire management *Sci. Adv.* **8** eabl7161
Price C 2009 Will a drier climate result in more lightning? *Atmos. Res.* **91** 479–84
Qin Y, Abatzoglou J T, Siebert S, Huning L S, AghaKouchak A, Mankin J S, Hong C, Tong D, Davis S J and Mueller N D 2020 Agricultural risks from changing snowmelt *Nat. Clim. Change* **10** 459–65
Quilcaille Y, Batibeniz F, Ribeiro A F S, Padrón R S and Seneviratne S I 2023 Fire weather index data under historical and shared socioeconomic pathway projections in the 6th phase of the coupled model intercomparison project from 1850 to 2100 *Earth Syst. Sci. Data* **15** 2153–77
Rodgers K B *et al* 2021 Ubiquity of human-induced changes in climate variability *Earth Syst. Dyn.* **12** 1393–411
Romps D M, Charn A B, Holzworth R H, Lawrence W E, Molinari J and Vollaro D 2018 CAPE times P explains lightning over land but not the land-ocean contrast *Geophys. Res. Lett.* **45** 12623–30
Romps D M, Seeley J T, Vollaro D and Molinari J 2014 Projected increase in lightning strikes in the United States due to global warming *Science* **346** 851–4
Scholten R C, Jandt R, Miller E A, Rogers B M and Veraverbeke S 2021 Overwintering fires in boreal forests *Nature* **593** 399–404
Screen J A and Simmonds I 2014 Amplified mid-latitude planetary waves favour particular regional weather extremes *Nat. Clim. Change* **4** 704–9
Senande-Rivera M, Insua-Costa D and Miguez-Macho G 2022 Spatial and temporal expansion of global wildland fire activity in response to climate change *Nat. Commun.* **13** 1208
Simpson I R *et al* 2023 The CESM2 single-forcing large ensemble and comparison to CESM1: implications for experimental design *J. Clim.* **36** 5687–711

Simpson I R, Seager R, Ting M and Shaw T A 2015 Causes of change in Northern Hemisphere winter meridional winds and regional hydroclimate *Nat. Clim. Change* **6** 65–70

Swart N C *et al* 2019 The Canadian earth system model version 5 (CanESM5.0.3) *Geosci. Model Dev.* **12** 4823–73

Tatebe H *et al* 2019 Description and basic evaluation of simulated mean state, internal variability, and climate sensitivity in MIROC6 *Geosci. Model Dev.* **12** 2727–65

Touma D, Stevenson S, Lehner F and Coats S 2021 Human-driven greenhouse gas and aerosol emissions cause distinct regional impacts on extreme fire weather *Nat. Commun.* **12** 212

Trapp R J, Diffenbaugh N S, Brooks H E, Baldwin M E, Robinson E D and Pal J S 2007 Changes in severe thunderstorm environment frequency during the 21st century caused by anthropogenically enhanced global radiative forcing *Proc. Natl Acad. Sci. USA* **104** 19719–23

Veraverbeke S, Rogers B M, Goulden M L, Jandt R R, Miller C E, Wiggins E B and Randerson J T 2017 Lightning as a major driver of recent large fire years in North American boreal forests *Nat. Clim. Change* **7** 529–34

Voelker S L, Wang S-Y S, Dawson T E, Roden J S, Still C J, Longstaffe F J and Ayalon A 2019 Tree-ring isotopes adjacent to Lake Superior reveal cold winter anomalies for the Great Lakes region of North America *Sci. Rep.* **9** 4412

Walker X J *et al* 2019 Increasing wildfires threaten historic carbon sink of boreal forest soils *Nature* **572** 520–3

Wang S Y S, Huang W R and Yoon J H 2015 The North American winter 'dipole' and extremes activity: a CMIP5 assessment *Atmos. Sci. Lett.* **16** 338–45

Wang S Y S, Yoon J-H, Becker E and Gillies R 2017 California from drought to deluge *Nat. Clim. Change* **7** 465–8

Wang S-Y, Hipps L, Gillies R R and Yoon J-H 2014 Probable causes of the abnormal ridge accompanying the 2013–2014 California drought: ENSO precursor and anthropogenic warming footprint *Geophys. Res. Lett.* **41** 3220–6

Wrona F J, Johansson M, Culp J M, Jenkins A, Mård J, Myers-Smith I H, Prowse T D, Vincent W F and Wookey P A 2016 Transitions in Arctic ecosystems: ecological implications of a changing hydrological regime *J. Geophys. Res. Biogeosci.* **121** 650–74

Young A M, Higuera P E, Duffy P A and Hu F S 2016 Climatic thresholds shape northern high-latitude fire regimes and imply vulnerability to future climate change *Ecography* **40** 606–17

Ziehn T, Chamberlain M A, Law R M, Lenton A, Bodman R W, Dix M, Stevens L, Wang Y-P and Srbinovsky J 2020 The Australian Earth System Model: ACCESS-ESM1.5 *J. South. Hemisph. Earth Syst. Sci.* **70** 193–214